Life Sciences 226 (2019) 117–129

Contents lists available at ScienceDirect

Life Sciences

journal homepage: www.elsevier.com/locate/lifescie

Neuroprotective effects of novel nanosystems simultaneously loaded with vinpocetine and piracetam after intranasal administration

Maha Nasr[a,*], Sara A. Wahdan[b]

[a] Department of Pharmaceutics and Industrial Pharmacy, Faculty of Pharmacy, Ain Shams University, Cairo, Egypt
[b] Department of Pharmacology and Toxicology, Faculty of Pharmacy, Ain Shams University, Cairo, Egypt

ARTICLE INFO

Keywords:
Nanocomposite
Microemulsion
Vesicles
Piracetam
Vinpocetine

ABSTRACT

Aims: The study aim was to test the efficacy of a novel created hybrid nanosystem compared to other nanosystems in treatment of scopolamine induced memory impairment.
Main methods: The fabrication and characterization of nanoformulations (microemulsion, liposomes, ethosomes, transfersomes and transethosomes) coencapsulating two cognitive enhancers; piracetam and vinpocetine delivered intranasally, in addition to a novel nanocomposite microemulsion/vesicular nanoformulation was described.
Key findings: Formulations delivered the drugs across sheep nasal mucosa, with cumulative percentage reaching 29.99% for vinpocetine and 57.78% for piracetam. While the solution form of the drugs was totally ineffective, the selected transethosomal, microemulsion and nanocomposite formulations reversed the scopolamine induced effect on the step through latency of passive avoidance test and the spontaneous alternation behavior in Y maze test, further confirmed by histopathlogical examination. All three nanoformulations significantly decreased the acetylcholinesterase activity and the extent of lipid peroxidation by 32–42%. The nanocomposite formulation was superior to the microemulsion and transethosomal formulations in its anti-inflammatory and antiapoptotic effects, delineated by higher extent of inhibition of COX-2 and caspase 3 expression respectively.
Significance: Results support the hypothesis that the novel microemulsion/vesicular nanocomposite system is a promising neuroprotective modality for intranasal brain targeting which is worthy of exploitation in other brain diseases.

1. Introduction

The blood brain barrier represents an extremely tight interface separating the brain from the vascular system, and is responsible for regulating the brain's microenvironment and for its protection [1]. Despite its integral role, it represents an obstacle when attempting to deliver drugs for treatment of brain diseases, which were reported to cause around 12% of total deaths worldwide [1].

Neurodegenerative diseases are among the most prevalent of all brain diseases, and unfortunately, their incidence is estimated to increase with time [2]. Among the commonly utilized drug categories for treatment of neurodegenerative diseases are nootropics. Two popular nootropic drugs exhibiting neuro- and glio-protective effects and reported to restore cognitive performance in dysfunctions caused by factors as hypoxia, hypoglcaemia and senile dementia of Alzheimer are vinpocetine and piracetam [3,4]. Piracetam is a cyclic derivative of GABA (gamma aminobutyric acid) which overcomes oxidative stress and reverses membrane changes that accompany Alzheimer's disease [5], and is used to treat dementia and prevent its progression [6]. Vinpocetine is a synthetic derivative of apovincamine, which treats vascular-based cerebral disorders [5]. It was also reported to treat senile dysfunction and Alzheimer's disease [7], and is very effective for memory enhancement owing to its cerebral vasodilator activity as well as its neuroprotective effect [8,9]. Despite the fact that both drugs are not FDA approved, they are still being used in several countries and were proven effective. They were utilized in the current study as model drugs of different properties to be tested for simultaneous loading; in which vinpocetine represents a lipophilic molecule while piracetam represents a hydrophilic molecule.

Since nootropics are known to act in the brain as their site of action, therefore bypassing the blood brain barrier is crucial. Therefore, in order to keep the balance between maintaining the brain protection

* Corresponding author at: Ain Shams University, Faculty of Pharmacy, Department of Pharmaceutics and Industrial Pharmacy, Monazamet El Wehda El Afrikia St., El Abbassia, Cairo, Egypt.
E-mail address: drmahanasr@pharma.asu.edu.eg (M. Nasr).

https://doi.org/10.1016/j.lfs.2019.04.014
Received 15 February 2019; Received in revised form 23 March 2019; Accepted 4 April 2019
Available online 11 April 2019
0024-3205/

conferred by the blood brain barrier and being able to deliver drugs efficiently across the blood brain barrier, non-invasive routes and new technologies were explored in the current era of research. Among the very common non-invasive routes of drug administration is the intranasal route. Not only is intranasal delivery advantageous in providing a shunt to the brain through the olfactory area, but it also overcomes the first pass metabolism and regional variability in oral absorption [10–12]. The latter advantage is particularly important for vinpocetine, since it's a sparingly soluble drug which suffers poor oral bioavailability (about 7%) because of first pass effect and pH dependant absorption [7,13,14].

In order to overcome the transmucosal barrier of the nose to reach the olfactory neurons, nanoparticles were highly sought in this regard, especially those containing surfactants [15]. Among the promising nanoparticulate systems used for intranasal delivery of drugs are microemulsions and vesicular systems. Microemulsions are thermodynamically stable systems characterized by their uniquely small particle size, consisting of oily and aqueous phases and stabilized by surfactant/cosurfactant [16,17]. Vesicular delivery systems are mainly composed of phospholipids constituting their outer bilayer, in addition to an aqueous internal core [18–22]. The aforementioned systems are unique in the sense that they contain both lipidic and aqueous domains within their structure, hence facilitating the simultaneous encapsulation of lipid and water soluble drugs. Based on the previous, the lipid soluble vinpocetine and the water soluble piracetam can be co-encapsulated in these systems, in order to benefit from their therapeutic synergy in the treatment of neurodegenerative diseases [23].

Therefore, the aim of the current manuscript was to prepare novel nanoparticulate systems co-encapsulating vinpocetine and piracetam; namely microemulsion and vesicular systems, in addition to a novel composite system described in the current paper; which is basically a hybrid of the microemulsion/vesicular systems. The prepared systems were physicochemically characterized, and tested for their pharmacological therapeutic efficacy in scopolamine- induced memory impairment model in rats, when administered *via* the intranasal route.

2. Materials and methods

2.1. Materials

Piracetam was kindly gifted by Misr Pharmaceutical Company, Egypt. Soyabean lecithin (Epikuron 200) was kindly provided by Cargill company, Germany. Vinpocetine, scopolamine, acetylthiocholine iodide, 5,5′-dithiobis-(2-nitrobenzoic acid) DTNB, HPLC grade methanol, HPLC grade chloroform, HPLC grade water, tween 20, tween 80, ethanol, phosphate citrate buffer tablets pH (5.5) were purchased from Sigma Aldrich (St. Louis, MO, USA).Potassium dihydrogen phosphate, disodium hydrogen phosphate and oleic acid were purchased from El Nasr pharmaceutical company, Egypt. NANOSEP tubes (100 kDa) were purchased from Pall company, USA. Uranyl acetate was purchased from Allied Signal, Germany. Antibodies and reagents' sources and IDs of antibodies and reagents are presented in the Supplementary material 1.

2.2. Preparation of vesicular systems, microemulsion, and the composite vesicular microemulsion system

A microemulsion system for vinpocetine and piracetam (F1) was prepared by the water dilution method [17,24,25]. Vinpocetine (25 mg) was dissolved in a mixture of ethanol, oleic acid and tween 20 according to the composition stated in Table 1 using magnetic stirring (Yellow line MAG HS7, IKA, France) followed by dropwise titration with water containing 100 mg piracetam. The chosen amounts were selected to form a clear microemulsion zone from a previously reported phase diagram prepared by other authors [26].

Different vesicular systems; namely liposomes, ethosomes, transfersomes and transethosomes (F2–F5) were prepared using the thin film hydration method [27–32], according to the compositions stated in Table 1. Two hundred milligrams of phospholipid and 25 mg vinpocetine were dissolved in a chloroform:methanol mixture of 2:1 v/v [18], followed by evaporation at 40 °C till the formation of a thin film (Janke and Kunkel, model RVO5-ST, IKA, Germany), and hydration using phosphate citrate buffer pH 5.5 containing 100 mg piracetam with rotation for 1 h at 150 rpm. In case of formulation F3, an amount of ethanol was included within the phosphate citrate buffer volume yielding ethosomes, while in case of formulation F4, an amount of tween 20 was included with the phospholipid yielding transfersomes. Formulation F5 was a hybrid of formulations F3 and F4; containing both tween 20 and ethanol, yielding transethosomes.

A novel composite microemulsion-vesicular system (F6) was prepared by first dissolving 200 mg phospholipid and 25 mg vinpocetine in chloroform:methanol mixture of 2:1 v/v, followed by hydration using 10 ml microemulsion formulation F1 containing 100 mg piracetam. Rotation was continued for 1 h at 150 rpm. Formulations F2–F6 were extruded five times through 400 nm filter (Nucleopore, Netherlands) using an extruder (Liposofast, Avestin, Germany) [33]. All formulations were kept at refrigeration temperature (4–8 °C) for further characterization.

2.3. Measurement of the particle size, polydispersity index (PDI) and surface charge of the formulations

The particle size, charge and PDI of the prepared formulations were measured following appropriate dilution using the Zetasizer device (NanoZS, Malvern, UK) [12,34,35].

2.4. Measurement of the entrapment efficiency (EE%) of vinpocentine

The entrapment efficiency of vinpocetine in the vesicular formulations F2–F5 and composite formulation F6 was calculated after centrifugal separation at 4000 rpm at 8 °C (Hermle cooling centrifuge, Germany) using Nanosep tubes [36]. An aliquot of the supernatant was diluted with methanol [37], and quantification of vinpocetine was done using HPLC (Agilent, USA) using C18 column (Eclipse XDB, 5 µm 4.6 × 150 mm, USA). The mobile phase was methanol:water 80:20 [9,38,39], flowing at 1.5 ml/min, and the drug was measured at wavelength 229 nm. The entrapment efficiency was calculated according to the following equation [18,40,41]:

$$EE\% = \frac{Entrapped\ drug}{Total\ drug\ amount} \times 100\%$$

EE% was only measured for vinpocetine since piracetam was present in the aqueous domains owing to its hydrophilicity [42].

2.5. Ex vivo permeation of the formulations across sheep nasal mucosa

In order to assess the permeation potential of the prepared formulations across nasal tissue, their *ex vivo* diffusion across sheep nasal mucosa was calculated. The mucosa was freshly obtained from a slaughterhouse, and cleaned before mounting between the donor and receptor compartments (1.77 cm^2) of a Franz diffusion device (VariomagTelesystem, Germany) [43]. The receptor compartment (of capacity 7.5 ml) contained phosphate buffer pH 7.4 including 2% tween 80 to ensure sink conditions for vinpocetine [7]. Two hundred microliters of each formulation were placed in the donor compartment, and samples were withdrawn from the receptor compartment at selected time intervals (10, 20, 30, 40, 60, 120, 240, 360 min) with replacement using fresh medium. The permeated vinpocetine and piracetam were quantified using the same HPLC method described previously for vinpocetine, but at a wavelength 215 nm for piracetam [44].

Table 1
Composition of different vinpocetine/piracetam formulations.

Formula code[a,b]	Type	Amount of tween 20 (ml)	Amount of oleic acid (ml)	Amount of ethanol (ml)	Amount of water (ml)	Amount of phosphate citrate buffer pH 5.5 (ml)	Amount of PC (mg)
F1	Microemulsion	4.1	0.28	0.3	5.3	–	–
F2	Liposomes	–	–	–	–	10	200
F3	Ethosomes	–	–	0.3	–	9.7	200
F4	Transfersomes	0.45	–	–	–	9.7	200
F5	Transethosomes	0.45	–	0.3	–	9.7	200
F6	Composite	4.1	0.28	0.3	5.3	–	200

[a] All formulations contained 25 mg vinpocetine and 100 mg piracetam.
[b] All formulations were completed to a total volume of 10 ml either with water for formulation 1 and 6 or with phosphate citrate buffer pH 5.5 for formulations F2–F5.

2.6. Stability assessment

The change in particle size, charge and polydispersity was recorded after three months of storage for all prepared formulations at refrigeration temperature, and was indicative of their stability [11,45].

2.7. Morphology visualization of selected formulations

Selected formulations were visualized for their morphology after negative staining with 2% uranyl acetate using transmission electron microscopy TEM (JEM-100 S, Japan) [18,35].

2.8. In vivo examination of selected formulations in scopolamine induced memory impairment model

Male Wistar rats weighing 200–250 g were purchased from the National Institute of Research (Cairo, Egypt). Rats were accommodated at a temperature of 25 °C with alternating 12 h light and dark cycles, and maintained on a standard diet pellet (El-Nasr, Abu Zaabal, Egypt) and water. Acclimatization of rats was done for days before conducting the experiment. The experimental protocol was approved by the research ethical committee of Faculty of Pharmacy, Ain Shams University, Egypt (REC-ASU-33).

A priori power analysis was conducted upon proposing the experimental model for determination of the sample size for each experiment. At significance level of 0.05, power of 80% and effect size 0.5, a sample size of 60 animals (10 in each group) would be required. Rats were randomly divided into 6 groups of 10 animals each and treated as follows; the first group was considered as the control group and given the vehicles: intranasal phosphate citrate buffer pH 5.5 + 2% tween 80, and intraperitoneal (i.p.) saline (0.9%) injections. The second group was given intranasal phosphate citrate buffer pH 5.5 + 2% tween 80, and intraperitoneal injection of scopolamine (SCO) at a dose of 2 mg/kg. The third group was given the intranasal solution of piracetam (PIR) and vinpocetine (VIN) (at the same concentrations present in the prepared formulations) dissolved in phosphate citrate buffer pH 5.5 using 2% tween 80 and SCO (2 mg/kg i.p.). The fourth, fifth and sixth groups received the selected formulations F5, F1, F6 (to be termed Nano 1, Nano 2 and Nano 3, respectively) intranasally and SCO (2 mg/kg, i.p.). The concentration of drugs in the nanoparticles as well as in the intranasal solution administered to group 3 was 10 mg/ml for PIR and 2.5 mg/ml for VIN. All formulations were given by intranasal route, 50 µl in each nostril, 90 min prior to SCO injection (2 mg/kg), for 8 consecutive days [46]. Behavioral tests were conducted 30 min after the last SCO injection [47]. The pharmacological experiments timeline is shown in Fig. 1.

At the end of the experiment, animals were euthanized by cervical dislocation. The whole brains of animals were taken out with dissection of hippocampi, followed by either storage at −80 °C for neurochemical analyses or fixation in 10% formalin solution for preparation of paraffin blocks, which were sectioned at 3 µm thickness by slide microtome, taking sections from 3 rats per group, with coordinates (1.6 to 2.8 mm and 0 to 1.2 mm posterior and anterior to the bregma respectively) for histological and immunohistochemical examinations [48].

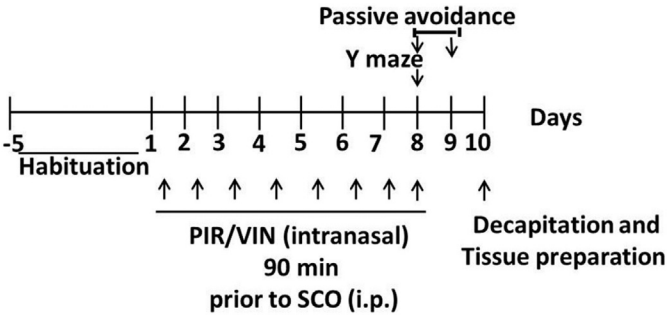

Fig. 1. Study timeline in terms of days of drugs administration, behavioral tests and tissue preparation.

2.9. Behavioral tests

2.9.1. Y maze test

Y maze was carried out in accordance with a previously described method [49]. The test is based on the principle that an animal must remember which arm it had entered previously to enable it to change (alternate) its choice on a following trial. The test is carried out in Y maze shaped apparatus with three arms. Each arm is labeled either A, B, or C and the rat was allowed to move for 8 min and its movement was recorded. Every time the rat enters an arm, with all of its limbs inside, its letter is written down. The number of alternations corresponds to the successive entries into 3 different arms in overlapping triplet sets. The total arm entries correspond to the total number of arms entered. The percentage alternation was calculated according to the equation:

$$\%\text{Alternation} = \frac{\textit{Number of alternations}}{\textit{Total number of arm entries} - 2} \times 100$$

2.9.2. Passive avoidance test

According to the theory of contextual fear conditioning used for assessment of memory changes, a step-through passive avoidance test was conducted (Ugo Basile, Italy) [50]. The device is composed of 2 compartments partitioned by an automatically sliding door; the first one is white and lit up by a 10-W bulb and the second is a black dark chamber whose grid floor delivers an electric shock of required intensity when stepped on by rats. Each rat was subjected to a training and a test session. In the training session (which was performed 30 min after the last SCO dose), each rat was placed in the first compartment. Upon stepping to the dark compartment, placing its four paws on the grid floor, the sliding door closed and an electric shock of 1 mA was delivered for 2 s to the rat. Rats failing to enter the dark chamber within 90 s were not included in the experiment.

The test session was carried out 24 h after the training session, in which rats were again individually placed in the first chamber and their latency to step through the second compartment was recorded, and considered as a step-through response to evaluate their memory acquisition after exposure to an aversive stimulus.

2.9.3. Histopathological examination

Brain samples of groups (1–6) were fixed in 10% formal saline for 24 h, followed by alcohol dehydration. The parrafinized sections were cut at 3 µm thickness using a sledge microtome, followed by hematoxylin and eosin staining for histopathological examination using a light microscope (Carl Zeiss Axiostar plus, Germany).

2.9.4. Assessment of lipid peroxidation product (malondialdehyde)

The hippocampal levels of the lipid peroxidation product malondialdehyde (MDA) were assessed using MDA assay kit (Biodiagnostics Co., Cairo, Egypt). Results were recorded as nanomoles of MDA/mg protein. The latter was assessed using a commercial kit (Spectrum diagnostics, Cairo, Egypt), and expressed as mg/ml.

2.9.5. Assessment of acetylcholinesterase (AChE) activity

Acetylcholinesterase (AChE) activity was measured according to a previously described method [51,52]. 2.9 ml of 0.1 mM sodium phosphate buffer (pH 8.0) was added to 50 µl of the tissue homogenate (10% w/v in 0.1 M phosphate buffer, pH 7.4) and incubated at 37 °C for 5 min, followed by addition of 40 µl of acetylthiocholine iodide (154.38 mM) and 10 µl of DTNB (10 mM). The formation of thionitrobenzoic acid was recorded at 412 nm for 150 s at 30 s intervals using UV spectrophotometer (UV–Vis. Shimadzu spectrophotometer 1601). The AChE activity was calculated by measuring the concentration of the produced thionitrobenzoic acid and expressed as nanomoles/min/mg protein.

2.9.6. Immunohistochemical detection of COX-2 and caspase 3

Paraffinized tissue sections of 3 µm thickness were rehydrated in xylene then in ethanolic solutions. The slides were then blocked using 5% bovine serum albumin (BSA) in tris-buffered saline for 2 h. The sections were then immunostained using one of the following primary antibodies: rabbit polyclonal caspase-3 antibodies or rabbit polyclonal COX-2 antibodies at a concentration of 1 µg/ml containing 5% BSA in tris-buffered saline and incubated at 4 °C till next day. After washing the sections with tris-buffered saline, they were incubated with goat anti-rabbit secondary antibodies, followed by rewashing with tris-buffered saline and incubation for 5–10 min in solution of 0.02% diaminobenzidine containing 0.01% hydrogen peroxide [53]. Counter staining was performed using hematoxylin, and the sections were examined using a light microscope (Carl Zeiss Axiostar plus, Germany) supplied with CCD camera (Carl Zeiss AxiocamICc 1, Germany). Pictures were captured for one section per rat from 3 rats per group, and the average number of stained (positive) cells across 10 non-overlapping fields was calculated. The optical density of the stained cells was calculated using Leica MDLSD image analysis software. The principle of quantitation depends on the density of the brown color of the positive stained cells. When the protein is highly expressed, there is more binding with its antibody which appears as strong brown color giving high value of optical density. With lower expression of the targeted protein a faint color appears and low value of optical density was obtained. Differences in color intensity were determined as difference in optical densities of the color among groups.

2.10. Statistical analysis

Statistical analyses were done using the software programs GraphPad Instat version 2.0, and GraphPad Prism version 5.0. Passive avoidance non-parametric data was presented as medians and interquartile range and analyzed by Kruskal–Wallis test followed by Dunn's *post hoc* test. Other behavioral and neurochemical data were presented as mean ± S.D. and analyzed by One-way ANOVA test followed by Tukey Kramer post test. P values lower than 0.05 were considered significant. Kolmogorov and Smirnov test (KS) was used to test the normality of the data. For *in vitro*, and *ex vivo* experiments, values were reported as mean ± S.D. of three individual batches.

3. Results and discussion

Microemulsions and vesicles are versatile delivery systems, composed of lipidic and aqueous entities. Therefore, they can act as universal delivery systems that can deliver both hydrophilic and hydrophobic drugs. The microemulsion formulation F1 was composed of oleic acid as the oily phase, titrated with water as aqueous phase, and stabilized by tween 20 as surfactant and ethanol as cosurfactant. Microemulsions prepared using non ionic surfactants and ethanolic cosurfactant were reported to be promising systems for intranasal delivery of drugs [10]. The vesicular systems prepared in the current work were composed of phospholipids as the lipidic phase, and titrated with buffer as the aqueous phase. Formulation F2 was the conventional liposomal formulation, while formulation F3 additionally contained ethanol (hence called ethosomes), and formulation F4 additionally contained tween 20 (hence called transfersomes). Formulation F5 contained both ethanol and tween 20 in its composition (transethosomes). Ethosomes and transfersomes were considered the second generation of vesicles, containing additional penetration enhancers which confer deformable traits to those vesicles, hence allowing better intranasal permeation [54,55]. Transethosomes were not tested before for intranasal delivery, and the current paper represents the first attempt of their use intranasally. Finally, a novel formulation (F6) was prepared in the current work, which is a nanocomposite form of microemulsion and vesicles, in which phospholipids were hydrated using microemulsion as aqueous phase instead of using buffer as hydration medium, hypothesizing that this formulation would combine the benefits of both vesicular systems and microemulsions for intranasal delivery, with an opaque nature in contrast to the translucent nature of the microemulsion (Fig. 2). The two selected cognitive-enhancer drugs for loading within our systems were the hydrophilic piracetam and the lipophilic vinpocetine, in order to test the versatility of the prepared systems in loading drugs of different solubility properties.

3.1. Measurement of the particle size, polydispersity index (PDI) and zeta potential of the formulations

The properties of the prepared vinpocetine/piracetam formulations

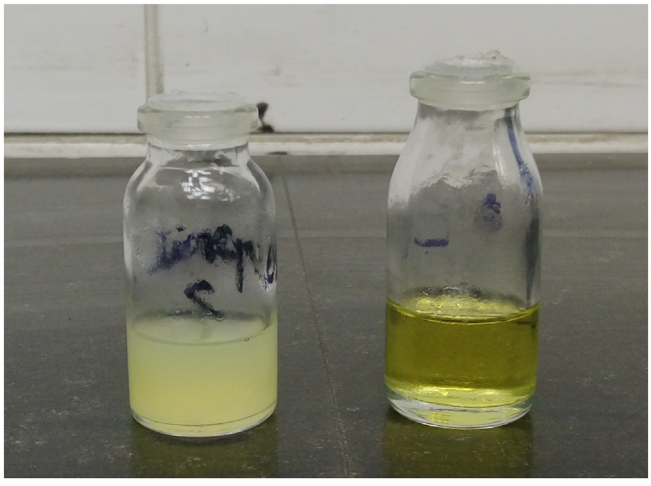

Fig. 2. Photograph of the microemulsion formulation (F1) on the right and the composite formulation F6 to the left.

Table 2
Characterization of different vinpocetine/piracetam formulations.

Formula code	Particle size (nm)	Zeta potential (mV)	PDI	EE% for vinpocetine	Cumulative permeated percent after 6 h for vinpocetine	Cumulative permeated percent after 6 h for piracetam	Particle size (nm) after 3 months storage	Zeta potential (mV) after 3 months storage	PDI after 3 months storage
F1	49.30 ± 5.24	−0.28 ± 0.04	0.39 ± 0.07	ND[a]	29.99 ± 2.02	57.78 ± 1.17	48.85 ± 2.99	−0.14 ± 0.36	0.41 ± 0.09
F2	402 ± 43	−28.5 ± 3.95	0.44 ± 0.28	88.32 ± 2.67	13.84 ± 0.26	29.26 ± 1.49	1118 ± 68.4	−26 ± 4.24	0.48 ± 0.13
F3	341 ± 49	−41.4 ± 3.76	0.41 ± 0.12	94.10 ± 0.14	17.95 ± 1.59	37.90 ± 5.22	788 ± 58	−36.7 ± 0.85	0.86 ± 0.12
F4	284 ± 6.61	−25.4 ± 1.06	0.38 ± 0.05	81.57 ± 2.98	23.44 ± 0.65	51.22 ± 9.15	350.7 ± 12.46	−20.5 ± 4.15	0.42 ± 0.03
F5	208 ± 9.25	−38 ± 0.43	0.39 ± 0.28	94.62 ± 2.09	26.12 ± 0.88	51.25 ± 2.30	214.4 ± 12.94	−37 ± 0.53	0.52 ± 0.07
F6	113 ± 3.47	−15.2 ± 0.46	0.27 ± 0.02	51.12 ± 0.95	28.68 ± 1.88	55.49 ± 2.20	121 ± 4.76	−14.1 ± 2.12	0.28 ± 0.02

Data was statistically analyzed using ANOVA followed by Tukey-Kramer as a post-hoc test, since the data represented in the table were confirmed to be normally distributed upon testing with Kolmogorov and Smirnov test.

[a] ND: not determined since all the amount of vinpocetine was loaded in the microemulsion, corresponding to 100% EE.

were measured using the Zetasizer device. As evident from the results displayed in Table 2, all formulations displayed a nanometer size range arranged in the following order: F2 > F3 > F4 > F5 > F6 > F1, and the One Way ANOVA test showed that differences were significant ($F(5,12) = 72.73$, at $P < 0.05$. The significantly smaller particle size exhibited by the microemulsion formulation F1 compared to other formulations could be attributed to its high content of the surfactant tween 20 and the cosurfactant ethanol [26]. The incorporation of ethanol in the ethosomal formulation (F3) didn't result in a significant difference from the particle size of the liposomes (F2), in which the increased viscosity of the formulation caused by ethanol/phospholipid interaction might have counteracted the fluidization ability of ethanol and its thinning potential on the phospholipid membrane [32]. However, the incorporation of tween 20 as edge activator in the transfersomal formulation (F4) resulted in a significant decrease in the particle size compared to liposomal formulation (F2), owing to its surface tension decreasing ability [56]. The concomitant addition of tween 20 with ethanol in the transethosomal formulation (F5) resulted in a further significant decrease in the particle size of the transfersomal formulation (F4), owing to the possible positive synergy created by double membrane fluidization and thinning by both tween 20 and ethanol. Upon creation of composite vesicles (F6) prepared by hydration of the phospholipid film by the microemulsion formulation instead of buffer, this resulted in a significant decrease in the particle size compared to all vesicles (F2–F5), which is attributed to the inclusion of some of the microemulsion formulation components being made of high surfactant/cosurfactant concentration within the phospholipidic bilayer of the vesicles, as well as the presence of microemulsion domains as the external aqueous dispersion medium and within the aqueous core of the vesicles (to be shown in the TEM section). The PDI of the formulations ranged from (0.27–0.44) suggesting all formulations were homogenous and moderately dispersed, especially that formulations F2–F6 were subjected to five extrusion cycles.

Regarding the zeta potential of the formulations, it ranged from (−0.28 to −41.4). The microemulsion formulation displayed the smallest zeta potential since it contained the non ionic surfactant tween 20 as its main component. The negative charge exhibited by the vesicles (F2–F5) is probably attributed to the negative charge of the phospholipids [36]. Formulations F3 and F5 containing ethanol exhibited the highest negative charge compared to other formulations, since ethanol is known to create a net negative charge [57]. The zeta potential of the composite formulation F6 exhibited a mid value between that of the microemulsion and the vesicles, since it contained a balanced amount of the negatively charged phospholipid and ethanol, and the neutral non ionic surfactant tween 20.

Therefore, the difference in composition of the nanoformulations was proven to affect their size, dispersity and charge properties.

3.2. Measurement of entrapment efficiency (EE%) of vinpocetine

Vinpocetine was totally solubilized in the microemulsion components (F1) owing to the presence of the surfactant tween 20 and ethanol, since vinpocetine is a poorly water soluble drug of log P 3.56 [58,59], which necessitated the use of surfactant/cosurfactant for its solubilization, corresponding to 100% EE% of vinpocetine within the microemulsion. The EE% of vinpocetine in the vesicles (F2–F5) ranged from 81.57 to 94.62% and differences among formulations were found to be statistically significant upon testing with One Way ANOVA F $(4,10) = 228.77$, at $P < 0.05$. This could be ascribed to the lipidic nature of the prepared vesicles, hence facilitating the encapsulation of the lipophilic vinpocetine within the lipidic bilayer. Upon further inspection of the results, it can be observed that the presence of ethanol (in ethosomal formulation F3 and transethosomal formulation F5) resulted in a significant increase in the entrapment efficiency of vinpocetine compared to other vesicles ($P < 0.05$). This came in accordance with other authors who attributed this to the increased solubility of

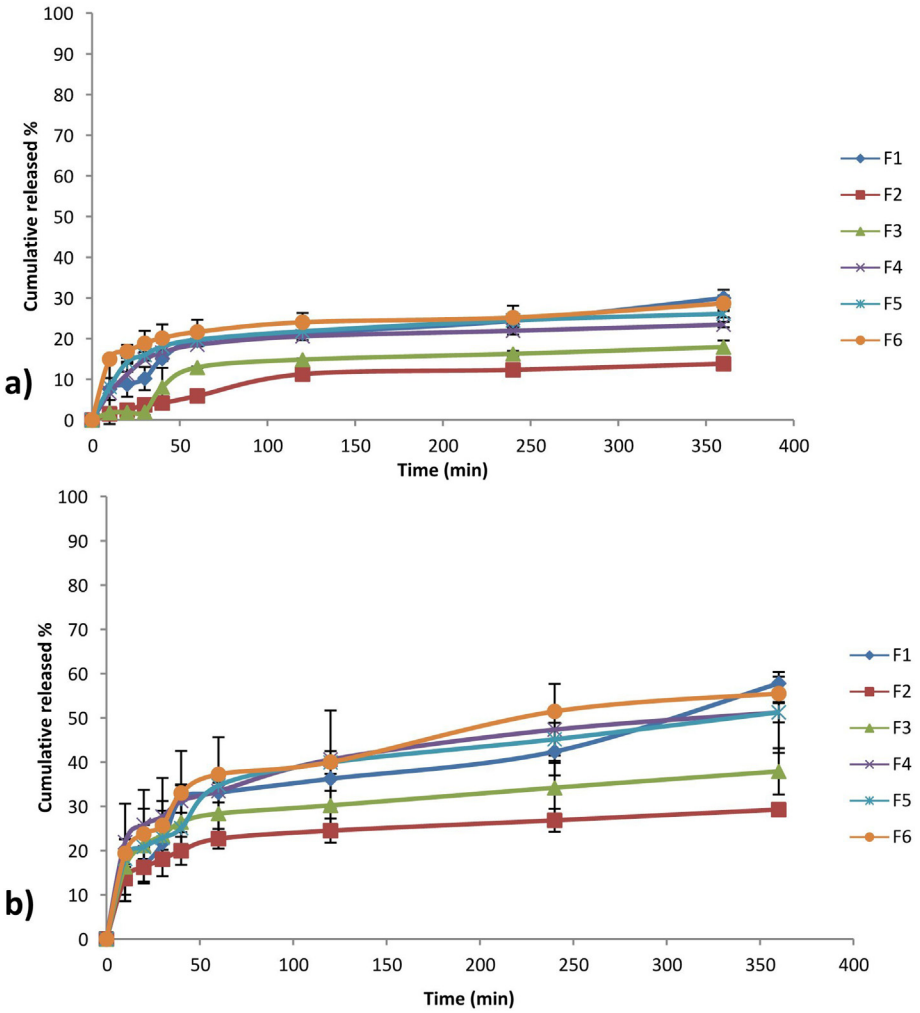

Fig. 3. Release profiles of different formulations for a) Vinpocetine b) Piracetam.

vinpocetine with the presence of ethanol [9]. Ethanol was known to associate itself within the lipidic bilayer, hence providing additional accommodating and solubilizing space for the lipophilic vinpocetine within the lipidic bilayer [60]. The presence of tween 20 only without ethanol in the F4 formulation resulted in the lowest EE% among vesicles, which could be attributed to the high HLB value of tween 20, previously reported to decrease the EE% of vinpocetine to a certain extent [37]. The EE% of the composite formulation F6 was 51.12%, since the external aqueous hydration phase was the microemulsion rather than the buffer, with high capability for solubilizing vinpocetine, leading to its presence in both the vesicular and microemulsion phases of the formulation.

3.3. Ex vivo permeation of formulations across sheep nasal mucosa

As shown in Table 2 and Fig. 3, different formulations displayed significantly different cumulative percent release for vinpocetine $F(5,12) = 63.05$ at $P < 0.05$ and piracetam $F(5,12) = 17.95$ at $P < 0.05$. The amount released of piracetam was double that released of vinpocetine for all formulations, which could be ascribed to the fact that piracetam resided in the outer external phase of the formulations, compared to vinpocetine which was encapsulated in the internal oily phase. Formulations F1, F4, F5 and F6 (microemulsion, transfersomes, transethosomes, composite system) displayed significantly higher released percent of piracetam and vinpocetine compared to the liposomal and ethosomal formulations. The former systems have in common that they contain tween 20 in their structure, which was reported to have high solubilizing power for hydrophobic solutes, leading to a concomitant increase in their release from vesicular systems [37]. Moreover, being tensioactive, tween 20 was reported to decrease the mucus viscosity and fluidize the nasal mucosal membrane [61]. Results showed that the prepared formulations allowed the permeation of both drugs across the nasal mucosa, and therefore, they can be considered promising for delivering the drugs to the brain upon permeation through the olfactory region. Given the high permeated amounts of both drugs across the nasal mucosa, the intranasal route was proven to be a successful route for administration of the prepared nanosystems.

3.4. Stability assessment

As shown in Table 2, formulations F1, F5, F6 displayed sufficient stability, manifested by insignificant variation in their particle size, PDI and surface charge values, while formulations F2, F3 and F4 were rather unstable and displayed significant increase in particle size upon storage, without general significant change in their PDI or zeta potential values. The tendency for aggregation upon storage for liposomal, ethosomal and transfersomal formulations was previously reported [18,62,63]. The stability of microemulsion came in accordance with other authors who reported the good shelf stability of microemulsions, manifested by no changes in their physicochemical parameters [64,65]. The better stability of transethosomes compared to other vesicles could be ascribed to the combined effect of tween 20 and ethanol in delaying the aggregation of the vesicles.

As evident from the previous studies, the microemulsion

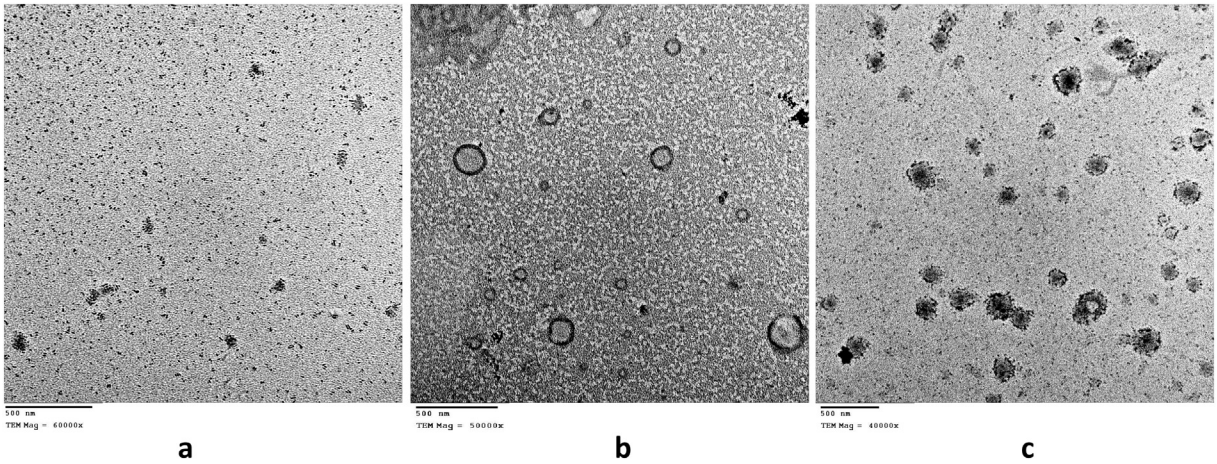

Fig. 4. TEM micrographs of the a) microemulsion formulation F1 b) transethosomal formulation F5 c) composite formulation F6.

formulation F1, the transethosomal formulation F5 and the composite formulation F6 displayed sufficient stability, in addition to high EE% of vinpocetine and increased permeated amount of both vinpocetine and piracetam across sheep nasal mucosa, and hence they were selected for further characterization.

3.5. Morphology visualization of selected formulations

As shown in Fig. 4, the microemulsion formulation F1 displayed small spherical droplet morphology, while the transethosomal formulation F5 displayed the typical vesicular morphology of a continuous lipid bilayer and an aqueous core. On the other hand, the composite formulation F6 displayed a hybrid morphology of the aforementioned formulations, in which they displayed a lipidic bilayer but was rather discontinuous, in addition to a microemulsion core, which confirms the ability of the microemulsion formulation to act as aqueous hydration medium for vesicles.

3.6. Behavioral tests

Male rats were used in the behavioral experiments in order to exclude the change in female sex hormones levels, which were reported to impact the behavioral parameters, since estrogen was previously reported to positively influence learning and memory in rats, as well as the cognitive functions within the mammalian brain.

The immediate working memory of rats was investigated by recording the spontaneous alternation attitude in Y-maze test (Fig. 5a). Applying Kolmogorov-Smirnov test showed the normality of the data of all groups, and the One-way ANOVA analysis showed a significant difference between groups ($F(5,31) = 16.1$, at $P < 0.05$). Results showed that SCO (2 mg/kg, i.p.) significantly reduced the spontaneous alternation percent by 46%. The solution form of PIR/VIN could not reverse SCO-induced effect on the percent of alternation between arms. On the other hand, Groups 4, 5 and 6 treated with the nanoformulations showed a significant improvement in the percentage spontaneous alternation by 100%, 74% and 88%, respectively, compared to both SCO-treated group and the group treated with conventional PIR/VIN combination, with no significant difference between the 3 nano-formulations ($P > 0.05$).

To further confirm the antiamnestic potential of the formulations on SCO-induced memory impairment, a step-through passive avoidance (PA) task was performed in different groups. Kolmogorov-Smirnov test showed that the data were not normally distributed, and hence were analyzed using non parametric test Kruskal-Wallis followed by Dunn's *post hoc* test. In the training session, no statistically significant difference was found in the step-through latency among between all groups (Fig. 5b).

On the other hand, in the test session, a statistically significant difference was found between groups (Fig. 5c). SCO administration significantly shortened the step-through latency by 83%, compared to the vehicle-treated group, which suggested clear memory impairment induced by SCO. Our findings came in accordance with previous studies which reported that administration of scopolamine impaired fear conditioning performance and spatial memory in rats [66,67]. Similar to what was encountered with the previous test, the solution form of the drugs (group 3) could not reverse SCO-induced effect on the step through latency. On the other hand, groups 4–6 treated with the nanoformulations showed a significant improvement in step through latency by 400%, 370% and 367%, respectively, compared to SCO-treated group. A significant amelioration in step-through latency for the 3 nanoformulations was observed ($P < 0.05$), compared to group 3, with no significant difference between the 3 nanoformulations ($P > 0.05$).

Results of the behavioral tests confirm the nasal penetration potential of the nanoformulations compared to the solution form, and their efficacy to reverse the induced amnesia/memory impairment by SCO.

3.7. Histopathological examination

In order to confirm these scopolamine-induced behavioral alterations, histopathological examination of brain specimens was performed for different treatment groups (Fig. 6). Brain samples taken from the control rats revealed no histopathological changes, with normal histological structure of the neurons in the cerebral cortex and fascia dentate in hippocampus. Treatment of rats with SCO (2 mg/kg) caused the appearance of nuclear pyknosis and neuronal degeneration in the cerebral cortex and fascia dentate of the hippocampus. Concurring with the results of the behavioral tests, the PIR/VIN administered in solution form could not reverse SCO-induced cerebral hippocampal alterations. Rats of group 4 treated with the transethosomal formulation caused a moderate amelioration in the brain histology, compared to SCO treated group, and showed mild nuclear pyknosis in the hippocampus, while rats of groups 5 and 6 treated with the microemulsion formulation and the composite formulation displayed normal histological appearance with no alterations in the cerebral cortex and hippocampus.

3.8. Assessment of acetylcholinesterase (AChE) activity and lipid peroxidation product (malondialdehyde) inSCO-treated rats

Acetyl choline (Ach) is the major neurotransmitter involved in the regulation of learning and memory functions [68], and cholinergic

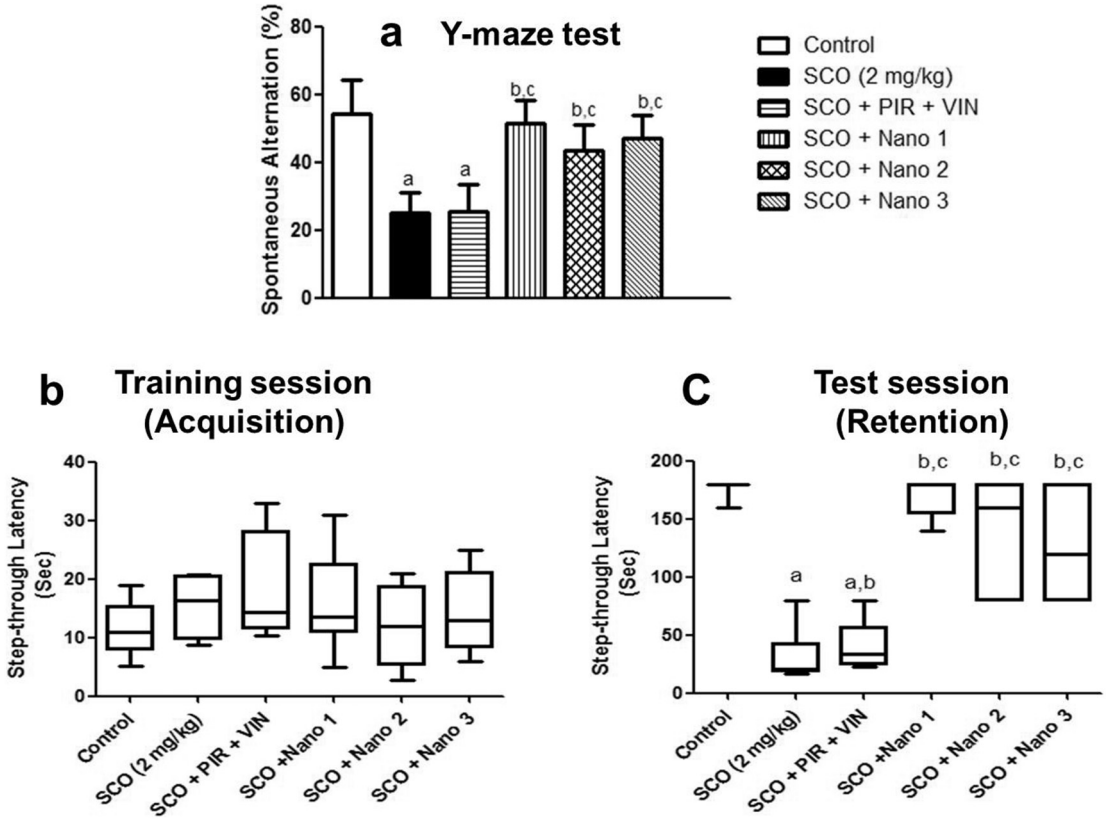

Fig. 5. Effect of different formulations of PIR/VIN on SCO-induced behavioral changes: a) Y maze b) Step-through passive avoidance. Data are presented as mean ± SD (n = 6–10). Weight of the animals (200–250 g).
[a]Significantly different from the control group, [b]Significantly different from SCO group, [c]Significantly different from group 3 treated with PIR/VIN solution at $P < 0.05$ using ANOVA followed by Tukey-Kramer as a post-hoc test at $P < 0.05$ for % Y maze test. Passive avoidance non-parametric data was presented as medians and interquartile range and analyzed by Kruskal–Wallis test followed by Dunn's *post hoc* test at $P < 0.05$.

neurodegeneration was found to be highly associated with cognitive impairment [69]. The concentration of acetylcholine in the brain is dynamically regulated by the activity of AChE [70], hence it was taken as a marker of cholinergic dysfunction. Kolmogorov-Smirnov test confirmed the normality of the data, and the One-way ANOVA analysis showed a significant difference between groups ($F(5,34) = 54.8$, at $P < 0.05$). As shown in Table 3, SCO administration increased acetyl cholinesterase (AChE) activity by 200%, compared to the vehicle treated group. This was in accordance with previous studies [71,72]. The solution form of PIR/VIN could not reverse SCO-induced elevation in AChE activity. On the other hand, treatment of rats with the transethosomal formulation Nano 1 significantly decreased AChE activity by 30%, while treatment with the microemulsion and nanocomposite formulations Nano 2 and Nano 3 respectively significantly reversed SCO-induced elevation in AChE activity by almost 60%, as compared to SCO-treated group, with no significant difference them ($P > 0.05$), indicating their comparable activity.

Besides cholinergic hypothesis in learning and memory, oxidative

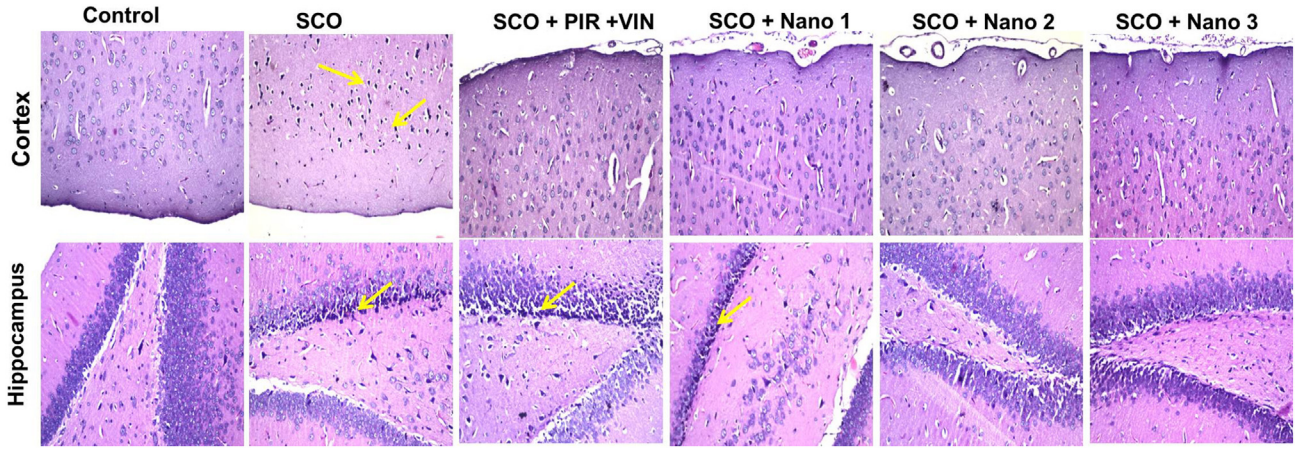

Fig. 6. Photomicrographs of H&E-stained rat hippocampal sections (×40) showing severe nuclear pyknosis and degeneration (yellow arrows) in the SCO-treated group and group treated with PIR/VIN solution in both cortex and hippocampus. Mild pyknosis and degeneration were also observed in group treated with the transethosomal formulation Nano 1. (For interpretation of the references to color in this figure legend, the reader is referred to the web version of this article.)

Table 3
Effect of different formulations of PIR/VIN on AChE activity and lipid peroxidation in SCO-treated rats.

Treated groups	AChE activity (nmol/min/mg protein)	MDA (nmol/mg protein)
Control	16.7 ± 6.2	12.3 ± 1.02
SCO (1 mg/kg)	52.6 ± 6.9[a]	25.6 ± 1.2[a]
SCO + PIR + VIN	45.2 ± 8.5[a]	20 ± 0.69[a,b]
SCO + Nano 1	36.5 ± 2.6[a,b]	11.4 ± 3.07[b,c]
SCO + Nano 2	17.6 ± 3.8[b,c,d]	13.5 ± 1.5[b,c]
SCO + Nano 3	17.1 ± 3.9[b,c,d]	11.6 ± 0.9[b,c]

Data are presented as mean ± SD (n = 6–10).
[a] Significantly different from the control group.
[b] Significantly different from SCO group.
[c] Significantly different from group 3 treated with PIR/VIN solution.
[d] Significantly different from group 4 at $P < 0.05$ using ANOVA followed by Tukey-Kramer as a post-hoc test, since the data represented in the table were confirmed to be normally distributed upon testing with Kolmogorov and Smirnov test.

stress is involved in the pathological characteristics of neurodegenerative disorders including AD [73]. Studies have proven that SCO-induced memory impairment in animal models was accompanied by increased oxidative stress in different brain areas [74,75]. In order to assess the effect of different formulations of PIR/VIN on hippocampal oxidative stress status, we determined the extent of lipid peroxidation in terms of malondialdehyde (MDA) assessment. Kolmogorov-Smirnov test confirmed the normality of the data, and the One-way ANOVA analysis showed a significant difference between groups ($F(5,25) = 66.1$, at $P < 0.05$). Administration of SCO significantly triggered a pro-oxidant effect as evidenced by 100% elevation in MDA level, compared to the vehicle-treated group. This came in accordance with previous studies which proved that increased lipid peroxidation and depletion of antioxidant defenses can play a major role in SCO-induced cognitive impairment [76,77]. In contrast, all treated groups showed a significant decrease in lipids peroxidation. Compared to the solution form of PIR/VIN (group 3), the 3 nanoformulations significantly decreased the extent of lipid peroxidation by 43%, 32% and 42%, respectively, with no significant difference between them ($P > 0.05$). The antioxidant effects of PIR and VIN were previously proven in a model of toxic demyelination of rat brain which was demonstrated by hindering lipid peroxidation increasing antioxidant enzymes [78].

3.9. Immunohistochemical detection of COX-2 and caspase 3

Neuroinflammation plays a critical role in SCO-induced cognitive impairment [79]. As shown in Fig. 7, we determined COX-2 protein expression by immunohistochemical technique. Control rats showed almost negative immunostaining which is confirmed by showing minimal optical density. The SCO-treated group displayed a significant increase in COX-2 protein expression in hippocampal tissue, as compared to the control group, which was evident from the intense brown staining. Kolmogorov-Smirnov test confirmed the normality of the data, and One-way ANOVA analysis showed a significant difference between groups ($F(5,34) = 89.9$, at $P < 0.05$) with optical density quantitation. This was in agreement with previous work showing significant elevation of inflammatory mediators like COX1, COX2 and IL-1β [80]. Treatment with the solution form of PIR/VIN could not reverse SCO-induced elevation in COX-2 protein expression showing an intense brown color. The transethosomal formulation Nano 1 showed only moderate immunostaining, while treatment with the microemulsion and composite formulations (Nano 2 and Nano 3) respectively showed minimal immunostaining as compared to the treatment with SCO alone or with groups 3 and 4. Moreover, the composite formulation Nano 3 could completely eliminate the effect of SCO on COX-2 expression showing a significant effect compared to the microemulsion formulation Nano 2. The quantitation was done by measuring the optical density across 10 different fields for each rat section, concluding that the nanocomposite formulation Nano 3 exhibited the highest anti-inflammatory effect compared to the other nanoformulations.

Neuronal apoptosis is another critical process affecting learning and memory [81,82]. It was proven that the key executioner of apoptosis; caspase-3 was able to induce neuronal dysfunction [83]. As shown in Fig. 8, we determined caspase 3 protein expression by immunohistochemical technique. Control rats showed almost negative immunostaining which is confirmed by showing minimal optical density. On the other hand, SCO-treated group showed a significant increase in caspase 3 protein expression in hippocampal tissue compared to the control group, which was evident from the intense brown staining. Kolmogorov-Smirnov test confirmed the normality of the data, and the One-way ANOVA analysis showed a significant difference between groups ($F(5,38) = 47.1$, at $P < 0.05$) with optical density quantitation. This was in accordance with previous work showing the SCO-induced expression of pro-apoptotic markers and neuronal death [84]. Treatment with the solution form of PIR/VIN could not reverse SCO-induced elevation in caspase 3 protein expression showing an intense brown color. The transethosomal formulation Nano 1 showed only moderate immunostaining, while treatment with either the microemulsion formulation Nano 2 or the nanocomposite formulation Nano 3 showed minimal immunostaining, as compared to the treatment with SCO alone or in combination with groups 3 or 4. As similarly encountered with the COX-2 assessment test, the nanocomposite formulation Nano 3 could completely eliminate the effect of SCO on caspase 3 expression showing a significant effect compared to the mere microemulsion Nano 2. The quantitation was done by measuring the optical density across 10 different fields for each rat section, concluding that the nanocomposite formulation exhibited the highest anti-apoptotic effect compared to the other nanoformulations.

The focus of this study was to test the hypothesis that nanoformulations composed of aqueous and lipophilic domains would be able to successfully co-load drugs of previously reported antiamnestic and learning enhancing capacities but of different lipophilicities, while exerting a therapeutic effect. Another focus was to conclude whether the use of intranasal route (which would maximally allow the administration of 100 µl of the formulation) would be an effective delivery modality or not, and this was also proven in the current work. The concentration of drugs in the nanoparticles was 10 mg/ml for PIR and 2.5 mg/ml for VIN and rats received a total 100 µl of the combination intranasally, compared to the large oral doses required from both drugs if administered *via* the oral route (piracetam given at a dose of 100 or 300 mg/kg and vinpocetine at a dose of 10 or 20 mg/kg).

To recapitulate, the formulation of piracetam and vinpocetine in nanoparticulate forms allowed for the exhibition of their therapeutic activity when administered *via* the intranasal route. The three nanoformulations; transethosomes, microemulsion and nanocomposite formulation were therapeutically effective owing to their small particle size and enhanced transportation potential across the nasal mucosa [85]. However, the novel composite microemulsion/vesicular formulation displayed better therapeutic efficacy compared to the mere microemulsion or vesicles in terms of anti-inflammatory and anti-apoptotic activities, hence delineating them as a novel promising means of brain delivery.

4. Conclusions

Nanotechnology has proven very effective in providing means for enhancing the delivery of cognitive enhancers to the brain *via* the intranasal route. The novel nanocomposite formulation was shown to exhibit both favorable pharmaceutical as well as pharmacological properties, hence paving the way for more drug categories to be loaded within this system to exhibit various therapeutic functions.

Supplementary data to this article can be found online at https://

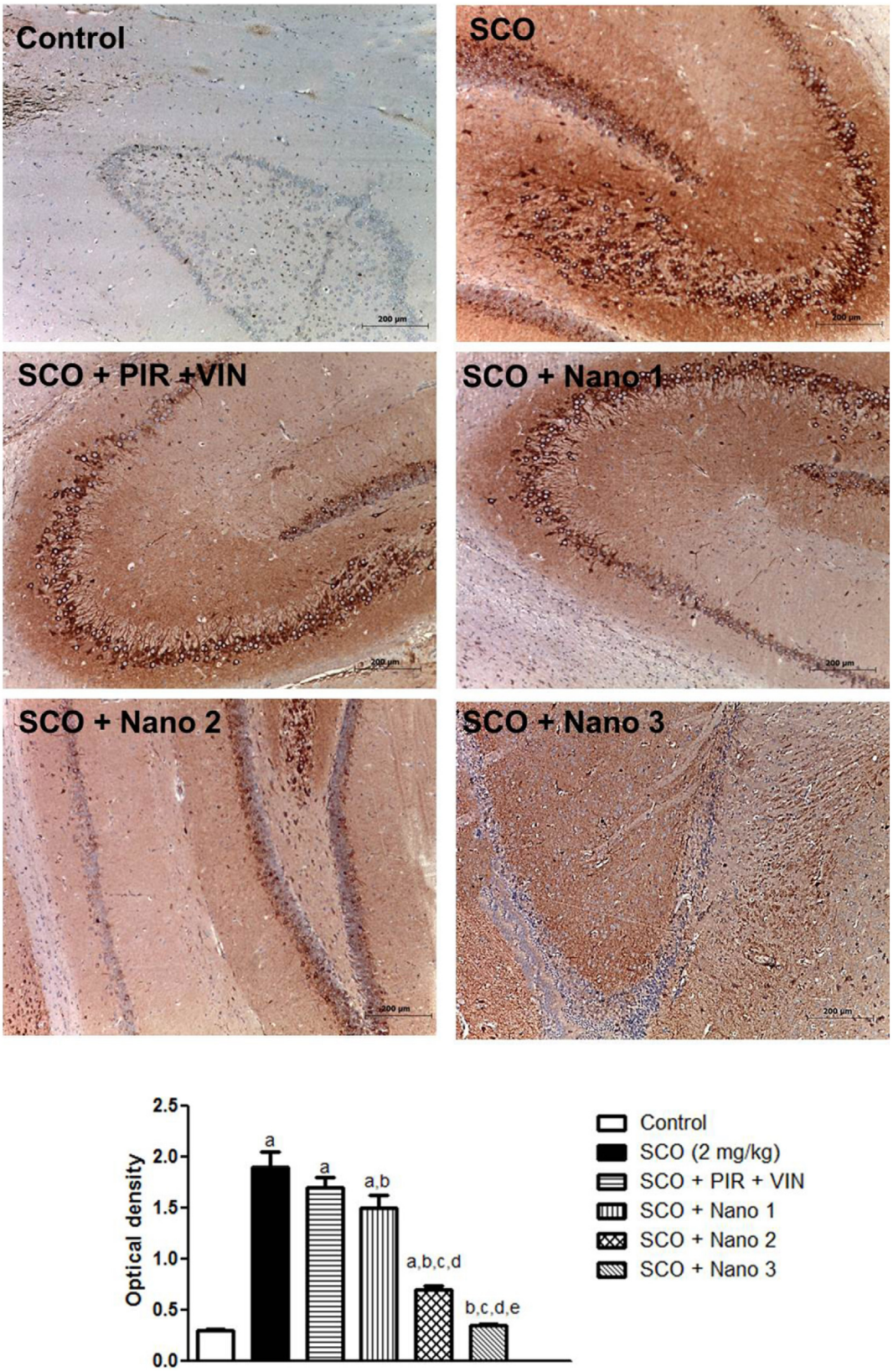

Fig. 7. Effect of different formulations on COX-2 expression in SCO-treated rats by immunohistochemical staining (magnification × 10). Quantitative image analysis for immunohistochemical staining expressed as optical densities across 10 different fields for each section (n = 3). Data are presented as mean ± SD. [a]Significantly different from the control group; [b]Significantly different from SCO group, [c]Significantly different from group 3 treated with PIR/VIN solution; [d]Significantly different from group treated with transethosomal formulation Nano 1; [e]Significantly different from group treated with the microemulsion formulation Nano 2, at $P < 0.05$ using ANOVA followed by Tukey-Kramer as a post-hoc test.

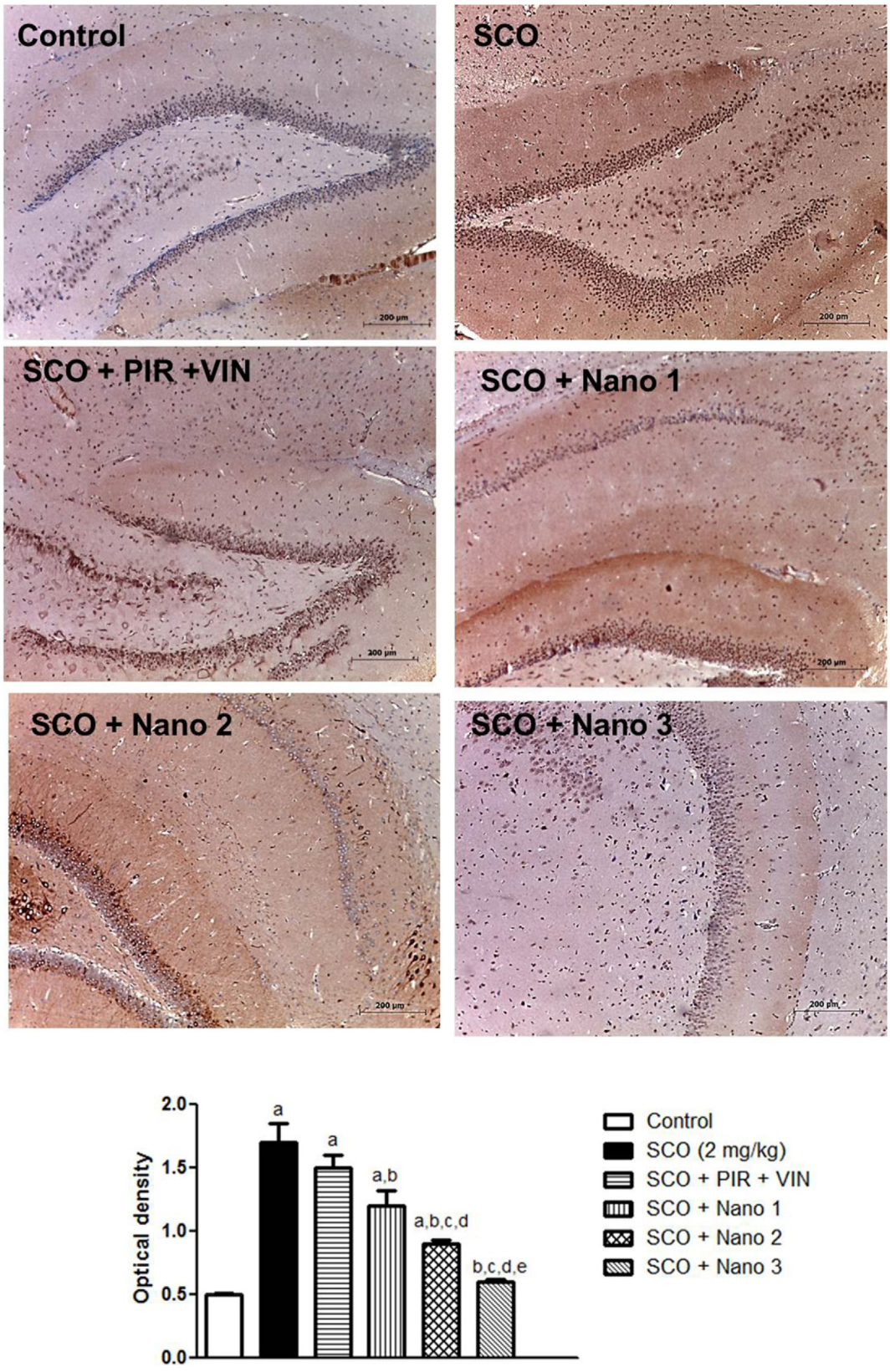

Fig. 8. Effect of different formulations on caspase 3 expression in SCO-treated rats by immunohistochemical staining (magnification × 10). Quantitative image analysis for immunohistochemical staining expressed as optical densities across 10 different fields for each section (n = 3). Data are presented as mean ± SD. [a]Significantly different from the control group; [b]Significantly different from SCO group, [c]Significantly different from group 3 treated with PIR/VIN solution; [d]Significantly different from group treated with transethosomal formulation Nano 1; [e]Significantly different from group treated with the microemulsion formulation Nano 2, at $P < 0.05$ using ANOVA followed by Tukey-Kramer as a post-hoc test.

doi.org/10.1016/j.lfs.2019.04.014.

Conflict of interests

The authors declare no conflicts of interest. No funding was provided for this manuscript.

References

[1] D. Furtado, M. Bjornmalm, S. Ayton, A. Bush, K. Kempe, F. Caruso, Overcoming the blood-barrier: the role of nanomaterials in treating neurological diseases, Adv. Mater. 30 (2018) e1801362.

[2] R. Brookmeyer, E. Johnson, K. Ziegler-Graham, H.M. Arrighi, Forecasting the global burden of Alzheimer's disease, Alzheimers Dement. 3 (2007) 186–191.

[3] B. Gabryel, M. Adamek, A. Pudelko, A. Malecki, H.I. Trzeciak, Piracetam and vinpocetine exert cytoprotective activity and prevent apoptosis of astrocytes in vitro in hypoxia and reoxygenation, Neurotoxicology 23 (2002) 19–31.

[4] M.G. Rao, B. Holla, S. Varambally, D. Raveendranathan, G. Venkatasubramanian, B.N. Gangadhar, Piracetam treatment in patients with cognitive impairment, Gen. Hosp. Psychiatry 35 (2013) 451e1–e6.

[5] P. Solanki, D. Prasad, S. Muthuraju, A.K. Sharma, S.B. Singh, G. Ilavzhagan, Preventive effect of piracetam and vinpocetine on hypoxia-reoxygenation induced injury in primary hippocampal culture, Food Chem.Toxicol. 49 (2011) 917–922.

[6] S.L. Evans, J.C. Brocklehurst, M.K. Palmer, Piracetam in chronic brain failure, Curr. Med. Res. Opin. 6 (1979) 351–357.

[7] R. Wang, Y. Xu, Development and evaluation of nanoparticles based on mPEG-PLA for controlled delivery of vinpocetine: in vitro and in vivo studies, Artif. Cells Nanomed. Biotechnol. 45 (2017) 157–162.

[8] L.S.S. Ribeiro, D.C. Ferreira, F.J.B. Veiga, Physicochemical investigation of the effects of water-soluble polymers on vinpocetine complexation with β-cyclodextrin and its sulfobutyl ether, Eur. J. Pharm. Sci. 20 (2003) 253–266.

[9] A.A. Moghaddam, M. Agil, F.J. Ahmad, M.M. Ali, Y. Sultana, A. Ali, Nanoethosomes mediated transdermal delivery of vinpocetine for management of Alzheimer's disease, Drug Deliv 22 (2015) 1018–1026.

[10] Q. Zhang, X. Jiang, W. Jiang, W. Lu, L. Su, Z. Shi, Preparation of nimodipine-loaded microemulsion for intranasal delivery and evaluation on the targeting efficiency to the brain, Int. J. Pharm. 275 (2004) 85–96.

[11] M.A. Mouez, M. Nasr, M. Abdel-Mottaleb, A.S. Geneidi, S. Mansour, Composite chitosan-transfersomal vesicles for improved transnasal permeation and bioavailability of verapamil, Int. J. Biol.Macromol. 93 (2016) 591–599.

[12] S.S. Barakat, M. Nasr, R.F. Ahmed, S.S. Badawy, S. Mansour, Intranasally administered in situ gelling nanocomposite system of dimenhydrinate: preparation, characterization and pharmacodynamic applicability in chemotherapy induced emesis model, Sci. Rep. 7 (2017) 9910.

[13] L. Ribeiro, D.C. Ferreira, F.J.B. Veiga, In vitro controlled release of vinpocetive-cyclodextrin-tartaric acid multicomponent complexes from HPMC swellable tablets, J. Control. Release 103 (2005) 325–339.

[14] C. Lin, F. Chen, T. Ye, L. Zhang, W. Zhang, D. Liu, W. Xiong, X. Yang, W. Pan, A novel oral delivery system consisting in “drug-in cyclodextrin-in nanostructured lipid carriers” for poorly water-soluble drug: vinpocetine, Int. J. Pharm. 465 (2014) 90–96.

[15] L. Battaglia, P.P. Panciani, E. Muntoni, M.T. Capucchio, E. Biasibetti, P. De Bonis, S. Mioletti, M. Fontanella, S. Swaminathan, Lipid nanoparticles for intranasal administration: application to nose-to-brain delivery, Expert Opin. Drug Deliv. 15 (2018) 369–378.

[16] R.M. Hathout, M. Nasr, Transdermal delivery of betahistine hydrochloride using microemulsions: physical characterization, biophysical assessment, confocal imaging and permeation studies, Colloids Surf. B Biointerfaces 110 (2013) 254–260.

[17] M. Nasr, S. Abdel-Hamid, N.H. Moftah, M. Fadel, A.A. Alyoussef, Jojoba oil soft colloidal nanocarrier of a synthetic retinoid: preparation, characterization and clinical efficacy in psoriatic patients, Curr. Drug Deliv. 14 (2017) 426–432.

[18] M. Nasr, S. Mansour, N.D. Mortada, A.A. Elshamy, Vesicular aceclofenac systems: a comparative study between liposomes and niosomes, J. Microencapsul. 25 (2008) 499–512.

[19] E.A. Bseiso, M. Nasr, O. Sammour, N.A. Abd El Gawad, Recent advances in topical formulation carriers of antifungal agents, Indian J. Dermatol. Venereol. Leprol. 81 (2015) 457–463.

[20] S. Hatem, M. Nasr, S.A. Elkheshen, A.A. Geneidi, Recent advances in antioxidant cosmeceutical topical delivery, Curr. Drug Deliv. 15 (2018) 953–964.

[21] S.S. Amer, M. Nasr, W. Mamdouh, O. Sammour, Insights on the use of nanocarriers for acne alleviation, Curr. Drug Deliv. 16 (2019) 18–25.

[22] R. Abdelgawad, M. Nasr, M.Y. Hamza, G.A.S. Awad, Topical and systemic dermal carriers for psoriasis, Int. J. Curr. Pharm. Res. 8 (2016) 4–9.

[23] R.T. Jadhav, P.H. Patil, P.R. Patil, Formulation an evaluation of bilayered tablet of piracetam and vinpocetine, J. Chem. Pharm. Res. 3 (2011) 423–431.

[24] M. Nasr, S. Abdel-Hamid, Optimizing the dermal accumulation of a tazarotene microemulsion using skin deposition modeling, Drug Dev. Ind. Pharm. 16 (2015) 322–332.

[25] S.A. Ramez, M.M. Soliman, M. Fadel, F. Nour-El-Deen, M. Nasr, E.R. Youness, D.M. Aboel-Fadl, Novel methotrexate soft nanocarrier/fractional erbium YAG laser combination for clinical treatment of plaque psoriasis, Artif. Cells Nanomed.Biotechnol. 46 (2018) 996–1002.

[26] L. Deng, F. Que, H. Wei, G. Xu, X. Dong, H. Zhang, Solubilization of tea seed oil in a food-grade water-dilutable microemulsion, PLoS One 10 (2015) e0127291.

[27] S. Hatem, M. Nasr, N.H. Moftah, M.H. Ragai, A.S. Geneidi, S.A. Elkheshen, Melatonin vitamin C-based nanovesicles for treatment of androgenic alopecia: design, characterization and clinical appraisal, Eur. J. Pharm. Sci. 122 (2018) 246–253.

[28] M. Fadel, K. Kassab, D.A. Abd El Fadeel, M. Nasr, N.M. El Ghoubary, Comparative enhancement of curcumin cytotoxic photodynamic activity by nanoliposomes and gold nanoparticles with pharmacological appraisal in HepG2 cancer cells and Erlich solid tumor model, Drug Dev. Ind. Pharm. 44 (2018) 1809–1816.

[29] A.M. Agiba, M. Nasr, S. Abdel-Hamid, A.B. Eldin, A.S. Geneidi, Enhancing the intestinal permeation of the chondroprotective nutraceuticals glucosamine sulphate and chondroitin sulphate using conventional and modified liposomes, Curr. Drug Deliv. 15 (2018) 907–916.

[30] R. Abdelgawad, M. Nasr, N.H. Moftah, M.Y. Hamza, Phospholipid membrane tubulation using ceramide doping "Cerosomes": characterization and clinical application in psoriasis treatment, Eur. J. Pharm. Sci. 101 (2017) 258–268.

[31] E.A. Bsieso, M. Nasr, N.H. Moftah, O.A. Sammour, N.A. Abd El Gawad, Could nanovesicles containing a penetration enhancer clinically improve the therapeutic outcome in skin fungal diseases? Nanomedicine (Lond.) 10 (2015) 2017–2031.

[32] E.A. Bseiso, M. Nasr, O.A. Sammour, N.A. Abd El Gawad, Novel nail penetration enhancer containing vesicles "nPEVs" for treatment of onychomycosis, Drug Deliv 23 (2016) 2813–2819.

[33] N.M. Aref, M. Nasr, R. Osman, Novel heat-stable enterotoxin (STa) immunogen based on cationic nanoliposomes: preparation, characterization and immunization, J. Vaccines Vaccin. 8 (2017) 1–8.

[34] M. Fadel, N. Samy, M. Nasr, A.A. Alyoussef, Topical colloidal indocyanine green-mediated photodynamic therapy for treatment of basal cell carcinoma, Pharm. Dev. Technol. 22 (2017) 545–550.

[35] M. Nasr, I. Taha, R.M. Hathout, Suitability of liposomal carriers for systemic delivery of risedronate using the pulmonary route, Drug Deliv 20 (2013) 311–318.

[36] S. Aldalaen, R.I. El-Gogary, M. Nasr, Fabrication of rosuvastatin-loaded polymeric nanocapsules: a promising modality for treating hepatic cancer delineated by apoptotic and cell cycle arrest assessment, Drug Dev. Ind. Pharm. 45 (2019) 55–62.

[37] H.M. El-Laithy, O. Shoukry, L.G. Mahran, Novel sugar esters proniosomes for transdermal delivery of vinpocetine: preclinical and clinical studies, Eur. J. Pharm. Biopharm. 77 (2011) 43–55.

[38] A. AbdElbary, N. Foda, O. El-Gazayerly, M. El Khatib, Reversed phase liquid chromatographic determination of vinpocetine in human plasma and its pharmacokinetic application, Anal. Lett. 35 (2002) 1041–1054.

[39] S. Nie, J. Wu, H. Liu, W. Pan, Y. Liu, Influence of admixed citric acid and physiological variables on the vinpocetine release from sodium alginate compressed matrix tablets, Drug Dev. Ind. Pharm. 37 (2011) 954–962.

[40] M. Nasr, S. Mansour, N.D. Mortada, A.A. El Shamy, Lipospheres as carriers for topical delivery of aceclofenac: preparation, characterization and in vivo evaluation, AAPS PharmSciTech 9 (2008) 154–162.

[41] R. Said-Elbahr, M. Nasr, M.A. Alhnan, I. Taha, O. Sammour, Nebulizable colloidal nanoparticles co-encapsulating a COX-2 inhibitor and a herbal compound for treatment of lung cancer, Eur. J. Pharm. Biopharm. 103 (2016) 1–12.

[42] A. Curticapean, S. Imre, New validated method for piracetam HPLC determination in human plasma, J. Biochem. Biophys. Methods 69 (2007) 273–281.

[43] M. Nasr, Development of an optimized hyaluronic acid-based lipidic nanoemulsion co-encapsulating two polyphenols for nose to brain delivery, Drug Deliv 23 (2016) 1444–1452.

[44] A.D. Lestari, A.T. Prasetyo, T. Palupi, E. Umayah, M. Yuwono, G. Indrayanto, HPLC determination of piracetam in tablets; validation of the method, J. Liq. Chromatogr. Relat. Technol. 28 (2005) 1407–1416.

[45] O. Ashraf, M. Nasr, M. Nebsen, A.M.A. Said, O. Sammour, In vitro stabilization and in vivo improvement of ocular pharmacokinetics of the multi-therapeutic agent baicalin: delineating the most suitable vesicular systems, Int. J. Pharm. 539 (2018) 83–94.

[46] M.D. Pandareesh, T. Anand, F. Khanum, Cognition enhancing and neuromodulatory propensity of Bacopa monniera extract against scopolamine induced cognitive impairments in rat hippocampus, Neurochem. Res. 41 (2016) 985–999.

[47] Y.J. Jang, J. Kim, J. Shim, C.Y. Kim, J.H. Jang, K.W. Lee, H.J. Lee, Decaffeinated coffee prevents scopolamine-induced memory impairment in rats, Behav. Brain Res. 15 (2013) 113–119.

[48] G. Paxinos, C. Watson, Atlas of the Rat Brain in Stereotaxic Coordinates, 3rd ed., Academic press, Sydney, 1986.

[49] E.J. Kim, I.H. Jung, T.K. Van Le, J.J. Jeong, N.J. Kim, D.H. Kim, Ginsenosides Rg5 and Rh3 protect scopolamine-induced memory deficits in mice, J. Ethnopharmacol. 146 (2013) 294–299.

[50] S.E. El-Agamy, A.K. Abdel-Aziz, S. Wahdan, A. Esmat, S.S. Azab, Astaxanthin ameliorates doxorubicin-induced cognitive impairment (chemobrain) in experimental rat model: impact on oxidative, inflammatory, and apoptotic machineries, Mol. Neurobiol. 55 (2018) 5727–5740.

[51] G.L. Ellman, K.D. Courtney, V. Andres Jr., R.M. Feather-Stone, A new and rapid colorimetric determination of acetylcholinesterase activity, Biochem. Pharmacol. 7 (1961) 88–95.

[52] E.T. Menze, A. Esmat, M.G. Tadros, A.B. Abdel-Naim, A.E. Khalifa, Genistein improves 3-NPA-induced memory impairment in ovariectomized rats: impact of its antioxidant, anti-inflammatory and acetylcholinesterase modulatory properties, PLoS One 10 (2015) e0117223.

[53] I.B. Buchwalow, W. Böker, Immunohistochemistry. Basics and Methods, 1st ed., Springer Science & Business Media USA, 2010, p. 156.

[54] H.M. Aboud, A.A. Ali, S.F. El-Menshawe, A.A. Elbary, Nanotransfersomes of carvedilol for intranasal delivery: formulation, characterization and in vivo evaluation,

Drug Deliv. 23 (2016) 2471–2481.
[55] S. Shelke, S. Shahi, K. Jadhav, D. Dhamecha, R. Tiwari, H. Patil, Thermoreversible nanoethosomal gel for the intranasal delivery of Eletriptan hydrobromide, J. Mater. Sci. Mater. Med. 27 (2016) 103.
[56] P. Muthuprasanna, N. Ravichandran, M. Manisha, Morphological influence of surfactants – span 20,40,80 and polysorbate 80 on conventional liposome, J. Pharm. Res. 5 (2012) 3571–3574.
[57] P. Verma, K. Pathak, Therapeutic and cosmeceutical potential of ethosomes: an overview, J. Adv. Pharm. Technol. Res. 1 (2010) 274–282.
[58] K. Mazak, J. Vamos, A. Nemes, A. Racz, B. Noszal, Lipophilicity of vinpocetine and related compounds characterized by reverse-phase thin-layer chromatography, J. Chromatogr. A 96 (2003) 195–203.
[59] L. Hua, P. Weisan, L. Jiayu, L. Hongfei, Preparation and evaluation of microemulsion of vinpocetine for transdermal delivery, Pharmazie 59 (2004) 274–278.
[60] I.M. Abdulbaqi, Y. Darwis, N.A.K. Khan, R.A. Assi, A.A. Khan, Ethosomal nanocarriers: the impact of constituents and formulation techniques on ethosomal properties, in vivo studies and clinical trials, Int. J. Nanomedicine 11 (2016) 2279–2304.
[61] M. Luisetti, E. Mevio, Evaluation of the fluidifying effect on nasal mucus of physiologic solution combined with increasing concentrations of polysorbates, Minerva Pediatr. 44 (1992) 427–430.
[62] T. Amnuaikit, T. Limsuwan, P. Khongkow, P. Boonme, Vesicular carriers containing phenylethyl resorcinol for topical delivery system; liposomes, tranfersomes and invasomes, Asian J. Pharm. Sci. 13 (2018) 472–484.
[63] H.N. Nugrahani, Iskandarsyah, Harmita, Stability study of azelaic acid proethosomes with lyoprotectant as stabilizer, J. Adv. Pharm. Technol. Res. 9 (2018) 61–64.
[64] L.C. Espinoza, M. Vacacela, B. Clares, M.L. Garcia, M.J. Fabrega, A.C. Calpena, Development of a nasal donepezil-loaded microemulsion for the treatment of Alzheimer's disease: in vitro and ex vivo characterization, CNS Neurol. Disord. Drug Targets 17 (2018) 43–53.
[65] V. Savic, M. Todosijevic, T. Ilic, M. Lukic, E. Mitsou, V. Papadimitriou, S. Avramiotis, B. Markovic, N. Cekic, S. Savic, Tacrolimus loaded biocompatible lecithin-based microemulsions with improved skin penetration: structure characterization and in vitro/in vivo performances, Int. J. Pharm. 529 (2017) 491–505.
[66] Y.J. Jang, J. Kim, J. Shim, C.Y. Kim, J.H. Jang, K.W. Lee, H.J. Lee, Decaffeinated coffee prevents scopolamine-induced memory impairment in rats, Behav. Brain Res. 245 (2013) 113–119.
[67] C.Y. Kim, G.Y. Lee, G.H. Park, J. Lee, J.H. Jang, Protective effect of arabinoxylan against scopolamine-induced learning and memory impairment, Biomol. Ther. (Seoul) 22 (2014) 467–473.
[68] P. Mohapel, G. Leanza, M. Kokaia, O. Lindvall, Forebrain acetylcholine regulates adult hippocampal neurogenesis and learning, Neurobiol. Aging 26 (2005) 939–946.
[69] M.E. Hasselmo, The role of acetylcholine in learning and memory, Curr. Opin. Neurobiol. 16 (2006) 710–715.
[70] P.E. Gold, Acetylcholine modulation of neural systems involved in learning and memory, Neurobiol. Learn. Mem. 80 (2003) 194–210.
[71] B.B. Lee, I. Shim, H. Lee, D.H. Hahm, Rehmannia glutinosa ameliorates scopolamine-induced learning and memory impairment in rats, J. Microbiol. Biotechnol. 21 (2011) 874–883.
[72] S.H. Kwon, H.K. Lee, J.A. Kim, S.I. Hong, H.C. Kim, T.H. Jo, Y.I. Park, C.K. Lee, Y.B. Kim, S.Y. Lee, C.G. Jang, Neuroprotective effects of chlorogenic acid on scopolamine-induced amnesia via anti-acetylcholinesterase and anti-oxidative activities in mice, Eur. J. Pharmacol. 649 (2010) 210–217.
[73] K. Jomova, D. Vondrakova, M. Lawson, M. Valko, Metals, oxidative stress and neurodegenerative disorders, Mol. Cell. Biochem. 345 (2010) 91–104.
[74] D.A. El-Sherbiny, A.E. Khalifa, A.S. Attia, Eel-D. Eldenshary, Hypericum perforatum extract demonstrates antioxidant properties against elevated rat brain oxidative status induced by amnestic dose of scopolamine, Pharmacol. Biochem. Behav. 76 (2003) 525–533.
[75] E.J. Jeong, K.Y. Lee, S.H. Kim, S.H. Sung, Y.C. Kim, Cognitive-enhancing and antioxidant activities of iridoid glycosides from Scrophularia buergeriana in scopolamine-treated mice, Eur. J. Pharmacol. 588 (2008) 78–84.
[76] K. Skalicka-Wozniak, B. Budzynska, G. Biala, A. Boguszewska-Czubara, Scopolamine-induced memory impairment is alleviated by xanthotoxin: role of acetylcholinesterase and oxidative stress processes, ACS Chem. Neurosci. 9 (2018) 1184–1194.
[77] C. Guo, J. Shen, Z. Meng, X. Yang, F. Li, Neuroprotective effects of polygalacic acid on scopolamine-induced memory deficits in mice, Phytomedicine 23 (2016) 149–155.
[78] O.M. Abdel-Salam, Y.A. Khadrawy, N.A. Salem, A.A. Sleem, Oxidative stress in a model of toxic demyelination in rat brain: the effect of piracetam and vinpocetine, Neurochem. Res. 36 (2011) 1062–1072.
[79] G. Karthivashan, S.Y. Park, M.H. Kweon, J. Kim, M.E. Haque, D.Y. Cho, I.S. Kim, E.A. Cho, P. Ganesan, D.K. Choi, Ameliorative potential of desalted Salicornia europaea L. extract in multifaceted Alzheimer's-like scopolamine-induced amnesic mice model, Sci. Rep. 8 (2018) 7174.
[80] A. Ahmad, K. Ramasamy, S.M. Jaafar, A.B. Majeed, V. Mani, Total isoflavones from soybean and tempeh reversed scopolamine-induced amnesia, improved cholinergic activities and reduced neuroinflammation in brain, Food Chem. Toxicol. 65 (2014) 120–128.
[81] M. Jahanshahi, E.G. Nickmahzar, F. Babakordi, The effect of Ginkgo biloba extract on scopolamine-induced apoptosis in the hippocampus of rats, Anat. Sci. Int. 88 (2013) 217–222.
[82] X.Q. Hou, D.W. Wu, C.X. Zhang, R. Yan, C. Yang, C.P. Rong, L. Zhang, X. Chang, R.Y. Su, S.J. Zhang, W.Q. He, Z. Qu, S. Li, Z.R. Su, Y.B. Chen, Q. Wang, S.H. Fang, Bushen-Yizhi formula ameliorates cognition deficits and attenuates oxidative stress-related neuronal apoptosis in scopolamine-induced senescence in mice, Int. J. Mol. Med. 34 (2014) 429–439.
[83] Y.F. Qian, H. Wang, W.B. Yao, X.D. Gao, Aqueous extract of the Chinese medicine, Danggui-Shaoyao-San, inhibits apoptosis in hydrogen peroxide-induced PC12 cells by preventing cytochrome c release and inactivating of caspase cascade, Cell Biol. Int. 32 (2008) 304–311.
[84] B. Saikia, C.C. Barua, J. Sarma, P. Haloi, S.M. Tamuli, D.J. Kalita, A. Purkavastha, A.G. Barua, Zanthoxylum alatum ameliorates scopolamine-induced amnesia in rats: behavioral, biochemical, and molecular evidence, Indian J. Pharmacol. 50 (2018) 30–38.
[85] A. Kumar, A.N. Pandey, S.K. Jain, Nasal nanotechnology: revolution for efficient therapeutics delivery, Drug Deliv 23 (2016) 681–693.